Fractionation and Characterization of an Ethylene–Propylene Copolymer Produced with a $MgCl_2/SiO_2/TiCl_4$/Diester-Type Ziegler–Natta Catalyst

Qi Dong,[1,2] Zhi-Qiang Fan,[1,2] Zhi-Sheng Fu,[1,2] Jun-Ting Xu[1,2]

[1]*Department of Polymer Science and Engineering, Zhejiang University, Hangzhou 310027, China*
[2]*Key Laboratory of Macromolecular Synthesis and Functionalization, Ministry of Education, Hangzhou 310027, China*

Received 15 September 2006; accepted 11 March 2007
DOI 10.1002/app.26552
Published online 10 October 2007 in Wiley InterScience (www.interscience.wiley.com).

ABSTRACT: An ethylene–propylene copolymer synthesized with a Ziegler–Natta catalyst was fractionated by a combination of dissolution/precipitation and temperature-gradient extraction fractionation. The fractions were characterized with ^{13}C-NMR, differential scanning calorimetry, and wide-angle X-ray diffraction. The fractionation was carried out mainly with respect to the content of ethylene, but the crystallizable propylene sequences could also exert an influence on the fractionation. The copolymer contained a series of components with wide variations in the compositions. With an increase in the ethylene content, the structure of the fractions became blockier and blockier, and the fraction extracted at 111°C had the blockiest structure. A further increase in the ethylene content led to a decrease in the length and number of the propylene sequences. Differential scanning calorimetry results showed that the composition distribution in single fractions was not homogeneous, and multiple melting peaks were observed. Wide-angle X-ray diffraction results revealed both polyethylene and polypropylene crystals in most of the fractions. Short propylene sequences could be included in the polyethylene crystals, and short ethylene sequences could also be incorporated into the polypropylene crystals. The incorporation of propylene sequences into polyethylene crystals strongly depended on the sequence distribution and crystallization conditions. © 2007 Wiley Periodicals, Inc. J Appl Polym Sci 107: 1301–1309, 2008

Key words: fractionation of polymers; microstructure; polyolefins; Ziegler-Natta polymerization

INTRODUCTION

Ethylene–propylene (EP) copolymers with various molecular architectures are emerging as a new class of thermoplastic elastomers. EP copolymers can act as impact modifiers of polypropylene (PP) and usually form alloys with PP by mechanical blending or *in situ* blending, which are widely used in consumer, appliance, and automotive industries. EP copolymers have drawn more and more attention because of their industrial importance. The copolymer part of an *in situ* PP/EP blend is designed to have an ethylene content in the range of 40–65 mol %.[1] The improvement in the impact properties of the blend, versus those of the PP homopolymer, is related to the glass-transition temperature of the copolymer and the amount, molecular weight, and size of the dispersed copolymer phase, which in turn are related to the average composition and composition distribution of the EP copolymer.[2] Our earlier studies showed that blocky or segmented copolymers in *in situ* PP/EP blends act as compatibilizers between the PP matrix and EP random copolymer phase, whereas the random copolymer (or rubber) can markedly enhance the low-temperature impact strength of the blends because of its very low glass-transition temperature.[3] However, the differences and correlations between the structure of *in situ* PP/EP blends and that of EP copolymers have not been clarified.

Commercial EP copolymers are generally made with homogeneous vanadium-based and heterogeneous titanium-based Ziegler–Natta catalyst systems. In the last decades, metallocene catalysts have also been developed. It is commonly accepted that Ziegler–Natta catalysts have a plurality of active species.[4–7] During copolymerization, because these active species have different reactivity ratios toward ethylene and propylene and different stabilities, the incorporation ratio of the two comonomers in the propagating chain varies with time. Thus, copolymers prepared by heterogeneous catalysts often exhibit both intermolecular and intramolecular compositional heterogeneity, and the produced copolymers are actually mixtures and contain a range of components with different composition and sequence

Correspondence to: Z.-Q. Fan (fanzq@zju.edu.cn).
Contract grant sponsor: Major State Basic Research Programs; contract grant number: 2005CB623804.
Contract grant sponsor: China Petroleum & Chemical Corporation.

distributions. Many techniques have been developed to investigate the compositional heterogeneity of ethylene copolymers, such as thermal fractionation[8] and temperature-rising elution fractionation.[9,10]

Extensive research has been carried out to correlate the physical properties and mechanical performances with the chain structures of EP copolymers. In EP copolymers, both ethylene and propylene segments of sufficient length are crystallizable. On the other hand, each type of monomer unit is able to cause disruption in the crystallizability of the other. A few publications have reported that relatively random EP copolymers with ethylene contents in the range of 35–65 mol % show minimal crystallinity.[11–13] Beyond this range, long crystallizable ethylene or propylene sequences are present in the backbone, and the copolymers are more similar to their homopolymers, which behave as thermoplastic materials. More recently, plenty of experimental results have proved that propylene units can enter the lattice of orthorhombic polyethylene (PE) crystals,[14–17] whereas ethylene units can also be partially incorporated into PP lattices.[18] Unfortunately, most of the research has been focused on ethylene-rich or propylene-rich EP copolymers, and the structure–property relationship of copolymers with intermediate compositions has been scarcely reported.

In our previous work, the chemical composition distributions of a series of EP copolymers synthesized with supported titanium catalysts were studied by simple extraction fractionation.[19] The objective of this study was to investigate the chain structure and properties of the same kind of EP copolymer in more detail. An EP copolymer was synthesized with a high-yield $MgCl_2/SiO_2/TiCl_4$/diester-type supported catalyst. Through temperature-gradient extraction fractionation (TGEF), eight fractions with different compositions were collected. Experimental results from ^{13}C-NMR, differential scanning calorimetry (DSC), and wide-angle X-ray diffraction (WAXD) analysis of the fractions were examined.

EXPERIMENTAL

Preparation of the ethylene/propylene copolymer

The copolymerization was carried out in a 1-L autoclave equipped with a mechanical stirrer. A high-yield $MgCl_2/SiO_2/TiCl_4$/diester-type catalyst[20] (Ti content = 3 wt %) was used in the copolymerization, with diphenyldimethoxysilane as an external donor and a triethylaluminum/triisobutylaluminum mixture with a molar ratio of 25/75 used as a cocatalyst. The gaseous ethylene and propylene monomer were completely mixed in a container in a molar ratio of 2/3 in advance. The monomers were purified by passage through columns filled with Al_2O_3, a deoxidizing reagent, and a molecular sieve. *n*-Heptane was used as the polymerization medium, and it was dried before use on 4-Å molecular sieves. The copolymerization was performed as follows. The autoclave was evacuated and purged with nitrogen several times at 95°C. After 300 mL of *n*-heptane was added at 70°C, the monomer gas pressure was adjusted to 1.0 kg/cm^2. The *n*-heptane solution of the cocatalyst (Al/Ti = 200 mol/mol), the solution of the external donor (Si/Ti = 5 mol/mol), and the catalyst ([Ti] = 7.2×10^{-5} mol/L) were added to the reactor sequentially. Then, the pressure was raised to 3.0 kg/cm^{-2} and held constant by continuous feeding of the monomer gas mixture with a constant composition into the autoclave. After 30 min of the reaction at 70°C, the copolymerization was terminated by pouring the liquid phase into an excess of ethanol containing 5% HCl, filtration, and washing of the solid product with ethanol three times. Subsequently, the copolymer was dried *in vacuo* at 65°C for 12 h.

Fractionation of the ethylene/propylene copolymer

An approximately 15-g copolymer sample was completely dissolved in 800 mL of boiling *n*-octane and then was precipitated by gradual cooling of the solution to room temperature over 5 h. The insoluble part was separated from the solution by centrifugation. The soluble part was recovered from the solution by distillation of the solvent, and both parts were dried *in vacuo*. This procedure separated the crystalline copolymer fraction containing the crystallizable sequence from the amorphous ethylene/propylene random copolymer.

A modified Kumagawa extractor was used to carry out TGEF of the insoluble copolymer part.[21] *n*-Octane was used as the solvent to successively extract the sample at different controlled temperatures, from room temperature to around 125°C. An approximately 1.5-g sample was used, and the fractions were recovered by rotating evaporation and drying *in vacuo*.

Characterization of the copolymer structure

^{13}C-NMR spectra of the fractions were measured on a Varian Mercury Plus 300 NMR spectrometer at 75 MHz. *o*-Dichlorobenzene-d_4 was used as a solvent, and the concentration of the polymer solution was 10 wt %. The spectra were recorded at 120°C with hexamethyldisiloxane as an internal reference. Chromium triacetylacetone (2–3 mg) was added to each sample to shorten the relaxation time and ensure the quantitative results.[3] Broadband decoupling with a pulse delay of 3 s was employed. Typically, 3000 transients were collected.

Thermal analysis of the polymer

An approximately 6–7-mg sample sealed in an aluminum crucible was used for the DSC measurements. All the fractions were pretreated by stepwise annealing; that is, the samples were first heated to 180°C and kept there for 10 min to eliminate the thermal history and then were quickly cooled to 150°C and maintained there for 12 h. The specimens were subsequently quenched to 140°C to carry out another 12-h run of isothermal crystallization. This procedure was repeated at every 10°C step to 50°C, and the treated samples were then stored for measurement at room temperature. Stepwise crystallization was conducted under a nitrogen atmosphere to avoid oxidation.

DSC analysis of the pretreated fractions was carried out with a TA Instrument model DSC Q100, which was calibrated for the temperature and melting enthalpy with indium as a standard. The heating scans were obtained through the heating of the thermal specimen from 30 to 180°C at a heating rate of 10/min.

WAXD

WAXD measurements were performed on a Rigaku D/max 2550PC rotating-anode X-ray diffractometer. The incident beam wavelength was 1.54 Å, which corresponded to 40 kV of Cu Kα radiation. The intensity profiles were obtained from radial averages of the scattering pattern intensities. Samples for WAXD were compression-molded into films approximately 0.3 mm thick and pretreated in a stepwise crystallization procedure, as described previously; they were then quenched with ice water and stored at room temperature for WAXD measurements. For comparison, samples without the stepwise crystallization treatment were also measured.

Measurements of the molecular weight

The molecular weights and molecular weight distributions of the EP copolymers were measured by gel permeation chromatography (GPC) in a PL 220 GPC instrument (Polymer Laboratories, Ltd.) at 150°C in 1,2,4-trichlorobenzene. Three PL mixed B columns ($500–10^7$) were used. Universal calibration against narrow polystyrene standards was adopted.

The intrinsic viscosity of the polymer fractions was determined at 130°C in an Ubbelohde viscometer with decalin as a solvent.

RESULTS AND DISCUSSION

Fractionation and characterization of the fractions

The fractionation included two steps: dissolution/precipitation fractionation of the overall copolymer sample followed by TGEF of the *n*-octane-insoluble part at room temperature.

On the basis of the well-known solubility and crystallization behavior of the thermoplastic polyolefins in solvents, the copolymer sample was first separated into two components by dissolution/precipitation fractionation: a soluble/amorphous fraction (a-EP) and an insoluble/crystalline fraction (c-EP), whose weight percentages were 71.80 and 28.20 wt %, respectively. These values were very close to the results of Randall,[22] who found the ratio of the amorphous EP copolymer to the crystalline EP copolymer to be nominally around 80/20 in such a copolymer with an intermediate composition range.

The ^{13}C-NMR spectra of the two EP copolymer fractions are given in Figure 1. All the resonance peaks were assigned with the terminology used by Carman and Wilkes;[23] the primary (methyl), secondary (methylene), and tertiary (methine) carbons were denoted P, S, and T, respectively. The composition was estimated from the spectrum according to the calculation scheme proposed by Randall.[22] The ethylene contents of the a-EP and c-EP fractions were found to be 42.70 and 67.88 mol %, respectively.

Further insights into sequence distributions can be obtained from reactivity ratios r_e and r_p. The product of the reactivity ratios, $r_e r_p$, can be used to describe the sequence distribution in copolymers: a value approaching zero is indicative of an alternating sequence, and a value of 1 is indicative of a statistical (Bernoullian) distribution of the comonomer, whereas a value larger than unity shows that the copolymer is either blocky or has a broad composition distribution. For this copolymer, the $r_e r_p$ value of the amorphous fraction is 1.81, whereas it is 8.54 for the

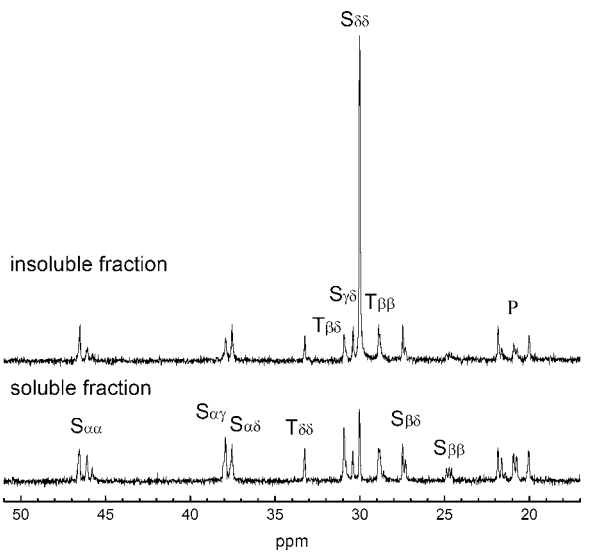

Figure 1 ^{13}C-NMR spectra of soluble and insoluble fractions at room temperature in *n*-octane.

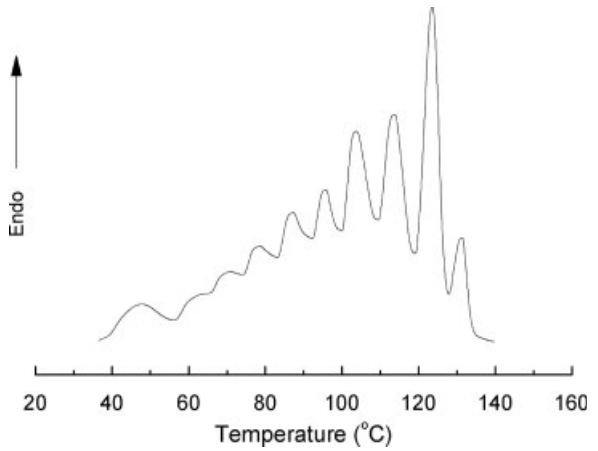

Figure 2 DSC curve of the crystalline fraction after stepwise crystallization.

crystalline fraction. This result shows that although the $r_e r_p$ values of the two fractions are larger than unity, the $r_e r_p$ value of the amorphous fraction is much closer to unity than that of the crystalline fraction. This means that the comonomer distribution of the amorphous fraction is almost random. So far, a judgment on the comonomer distribution of the crystalline fraction cannot be made simply with the value of $r_e r_p$ because such a large $r_e r_p$ value could be caused for two reasons: either the copolymer is extremely blocky, or it contains components with different comonomer distributions.

DSC measurements were carried out to investigate the composition heterogeneity of the crystalline fraction. The DSC heating curves of the crystalline fraction after stepwise annealing are shown in Figure 2.

Multiple melting peaks ranging from 35 to 135°C can be observed, and they were formed during the multistep isothermal crystallization. The broad melting range is a characteristic of Ti-based EP copolymers.[11] Each endotherm represents a population of crystals with almost the same thermodynamic stability and melting temperature. The differences among the endotherms are mainly caused by differences in the lamellar thickness of the crystal. Feng et al.[3] revealed that a blocky propylene–ethylene copolymer exhibits a complicated composition heterogeneity. From the DSC curve with multiple endotherms, we can qualitatively conclude that the crystalline fraction of the sample is an *in situ* blend of different polymer chains with different crystallizabilities.

A modified Kumagawa extractor was used to carry out TGEF of the crystalline fraction. Table I summarizes the TGEF results. For convenience, we have named the fractions according to the extraction temperature; for example, Fr111 represents the fraction extracted at 111°C. The c-EP component shows high intermolecular heterogeneity and comprises a number of copolymer fractions with different compositions. The fractions distribute rather uniformly in a temperature range of 92–125°C, and the ethylene content of the fractions increases with the extract temperature. Although the method of sample synthesis used in this work can cause broadening in the composition distribution of the copolymer, the broadening was estimated to be rather limited, as the copolymer yield was controlled at a low level. Therefore, the very broad composition distribution shown in Table I should be attributed to the presence of multiple active centers in the catalyst.[19] The molecular weight of the a-EP component is higher than that of the fractions in the c-EP component. Because the molecular weight of PE is usually higher than that of PP synthesized with the same catalyst, the lower molecular weight of the c-EP components, which have ethylene contents higher than those of the a-EP components, is hard to understand. A possible reason is that the fractions in the c-EP

TABLE I
TGEF Results for the Copolymer Samples

Fraction	Temperature (°C)[a]	wt %[b]	wt %[c]	Ethylene (mol %)	Intrinsic viscosity (dL/g)	M_w[d]	M_w/M_n[d]
Fr25	Room temperature		71.8^0	42.7	0.31	239,100	5.11
Fr58	58	5.5^0	1.5^5	—[e]	0.11	65,800	4.14
Fr82	82	11.9^2	3.3^6	47.1	0.14	95,300	4.44
Fr92	92	18.3^4	5.1^7	55.1	0.17	87,600	3.39
Fr103	103	19.7^6	5.5^7	74.7	0.14	65,800	3.01
Fr111	111	18.5^1	5.2^2	73.6	0.11	47,900	2.74
Fr121	121	11.0^6	3.1^2	76.5	0.13	72,400	3.59
Fr125	125	14.9^0	4.2^0	82.9	0.14	77,300	2.84

M_w, weight-average molecular weight; M_n, number-average molecular weight.
[a] Extraction temperature of the fractions.
[b] Normalized by the weight of c-EP.
[c] Normalized by the weight of the whole EP sample.
[d] Determined by GPC analysis.
[e] Not determined.

TABLE II
Compositions and Sequence Distributions of the Fractions Determined by ^{13}C-NMR

		Dyad distribution			Triad distribution								
Fraction	E	EE	EP	PP	EEE	EEP	PEP	EPE	PPE	PPP	$r_e r_p$	n_e	n_p
Fr25	42.7	22.5	42.0	35.5	13.8	17.3	11.5	9.3	24.9	23.0	1.81	2.0^3	2.7^3
Fr82	47.1	30.9	34.3	34.8	23.7	14.4	9.1	7.8	20.6	24.5	3.65	2.7^5	3.0^8
Fr92	55.1	43.8	26.4	29.8	37.9	12.0	5.3	6.4	17.4	21.1	7.52	4.1^8	3.4^1
Fr103	74.7	67.1	20.0	12.9	61.8	10.5	2.4	5.2	14. 5	5.6	8.59	7.4^5	2.5^2
Fr111	73.6	64.2	20.0	15.9	58.4	11.6	3.7	5.8	9.3	11.2	10.21	7.3^8	2.6^4
Fr121	76.5	69.3	20.3	10.4	64.4	9.9	2.3	6.0	14.2	3.3	7.0	7.5^5	2.3^2
Fr125	82.9	74.1	17.5	8.4	68.5	11.1	3.3	5.5	6.5	5.1	8.05	9.4^4	1.9^5

components were degraded during the extraction. The relatively small differences in the molecular weights of the c-EP fractions imply that the extraction was not dependent on the molecular weight.

To confirm the chain structures of the different fractions, ^{13}C-NMR spectra were recorded, and the data for the dyad and triad sequence distributions are listed in Table II, except for Fr58. The number-average sequence lengths of ethylene (n_e) and propylene (n_p) were derived as follows:

$$n_e = \frac{[\mathrm{E}]}{\frac{1}{2}[\mathrm{PE}]}$$

$$n_p = \frac{[\mathrm{P}]}{\frac{1}{2}[\mathrm{PE}]}$$

where E represents the ethylene unit and P represents the propylene unit. For the first three fractions extracted below 100°C, the contents of the [PPP] triad are similar but high. The contents of the [EEE] triad increase drastically with the extraction temperature. Meanwhile, the contents of the other triads, [EEP], [PEP], [EPE], and [PPE], which are caused by the alternation of ethylene and propylene units, decrease gradually as the extraction temperature increases. As a result, the lengths of the both ethylene and propylene sequences increase with the extraction temperature. This can also be seen from the changes in n_e, n_p, and $r_e r_p$. For the fractions extracted above 100°C, the content of the [PPP] triad is lower, whereas the content of the [EEE] triad is higher and increases gradually with the extraction temperature.

Examining the change in the microstructure with the extraction temperature, one can see that the fractionation is mainly based on the content of ethylene or the [EE] dyad. This means that the ethylene sequence is the key factor that determines the crystallization behavior of the fractions. However, under certain circumstances, crystallization of the propylene sequence also exerts an influence directly on the fractionation of the EP copolymer. For example, the ethylene content of Fr111 is slightly lower than that of Fr103, but the extraction temperature is higher than that of Fr103. This may be explained by the effect of the crystallization of the long propylene sequence on the fractionation.

Because the ethylene sequence is the major factor responsible for the crystallization behavior of the fractions, we will discuss the effect of the propylene sequence on the thermal properties and crystalline structure of the ethylene sequences. Before doing this, we must figure out how propylene sequences change in these fractions. On the basis of the ^{13}C-NMR data, the distribution of the propylene sequences in different fractions is schematically depicted in Scheme 1. In a-EP (Fr25), the lengths of both the propylene and ethylene sequences are very short, and both sequences exhibit weak crystallizability. As the extraction temperature increases, in F82 and Fr92, the number of short propylene sequences decreases, and the length of propylene sequences increases. Therefore, the structure becomes blockier and blockier. For Fr111, although the content of the [PPP] triad is lower than that of F82 or Fr92, the content of [EEE] is markedly increased, and it has the blockiest structure among all the fractions, as revealed by its large $r_e r_p$ value. With further increases in the ethylene content in the fractions, the number and length of the successive propylene sequences tend to decrease again.

Thermal properties of the fractions

Melting DSC traces of the fractions from the c-EP component are shown in Figure 3. The samples were

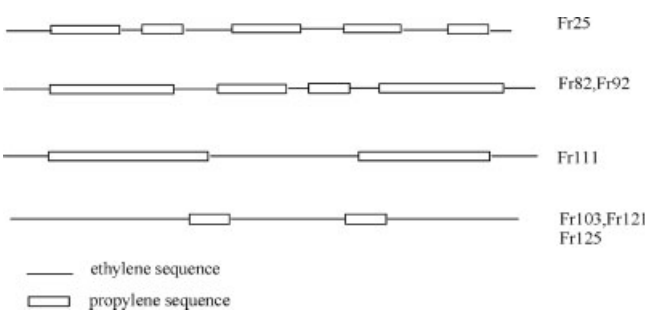

Scheme 1 Illustration of changes in the propylene sequence among the fractions.

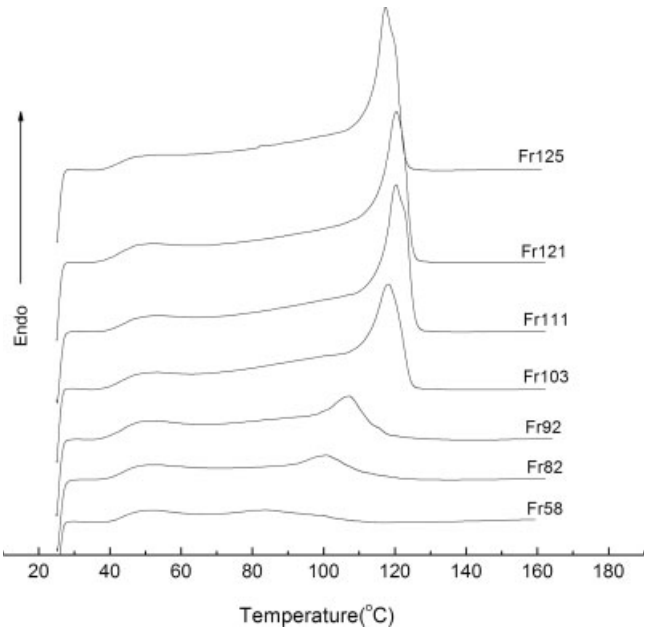

Figure 3 DSC melting thermograms of various fractions of the c-EP copolymer. All the samples were left at the ambient temperature over 2 weeks.

cooled from the melt in air and stored at the ambient temperature for 2 weeks before the DSC analysis. The first three fractions extracted below 100°C evidently have lower melting temperatures and crystallinity than the other fraction because of the lower ethylene contents of these fractions. There is no large difference in the melting temperatures for the fractions extracted above 100°C as the ^{13}C-NMR data show that these four fractions have ethylene contents close to one another. All the crystalline fractions show a common feature: there is a broad peak tail appearing in the low temperature range. In the DSC scans of the short-term nonisothermally crystallized samples, such a peak tail did not appear. Therefore, the peak tail can be attributed to the melting of short ethylene and propylene sequences, which form crystals only after long-time annealing at the ambient temperature.[11,24]

DSC experiments were also carried out for the fractions pretreated by stepwise crystallization. As shown in Figure 4, many sharp melting peaks are observed. Unlike the phenomena observed in the c-EP component, which is the mixture of these fractions, the multiple endotherms of each fraction mainly reflect intramolecular heterogeneity, which means that the multiple endotherms come from the melting of lamella formed by ethylene sequences of different lengths combined in the same polymer chain. As a result, from the number and intensity of the melting peaks, the intramolecular composition distribution can be qualitatively evaluated. Figure 4 shows that, with an increase in the extraction temperature, the number of crystallizable ethylene sequences becomes larger, and the length of the crystallizable ethylene sequences becomes longer.

Generally, thicker lamella are formed as the length of the ethylene sequences increases, and thus a higher melting temperature is observed. However, we noticed that the melting temperature of the peak appearing at the highest end of the peak series decreases with the average length of the ethylene sequences for the fractions extracted above 100°C after stepwise crystallization. The highest temperature (132.8°C) of an individual endotherm is found in Fr111, not in Fr125. Similar phenomena of melting-point depression can be seen in DSC curves of fractions that are annealed at the ambient temperature (see Fig. 3). As pointed out in the previous section, fraction Fr111 has the blockiest structure. We speculate that the melting peaks at 132.8°C in Fr111 and at 130.8°C in Fr103 result from the melting of crystallized propylene sequences. Because of the limitation in the length of the propylene sequences, the formed PP crystals have low melting temperatures, and the melting peaks overlap those of the PE crystals. Nevertheless, the effect of the molecular weight cannot be excluded completely. Fr111 has the lowest molecular weight, which may also facilitate the crystallization of PE and lead to a higher melting temperature.[25]

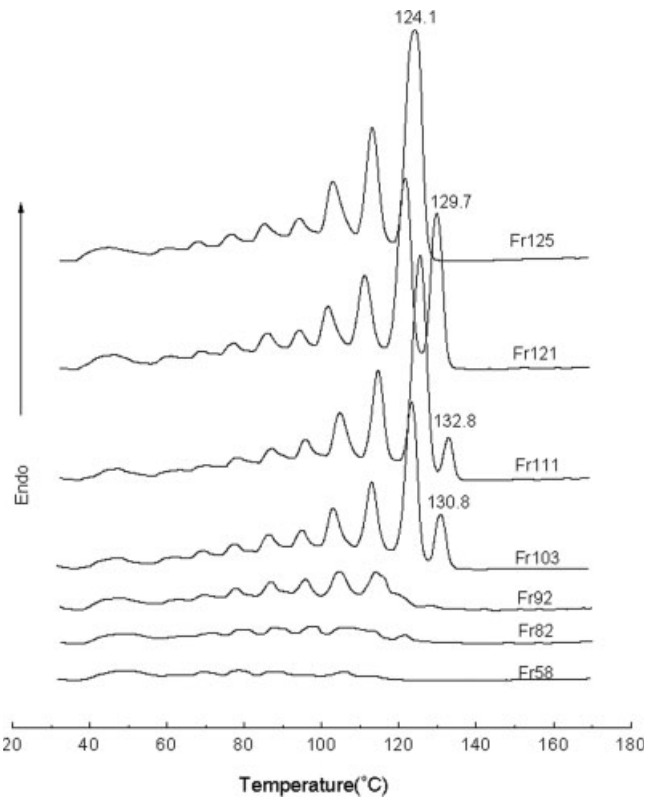

Figure 4 DSC melting traces of various fractions of the c-EP copolymer after a pretreatment by step crystallization.

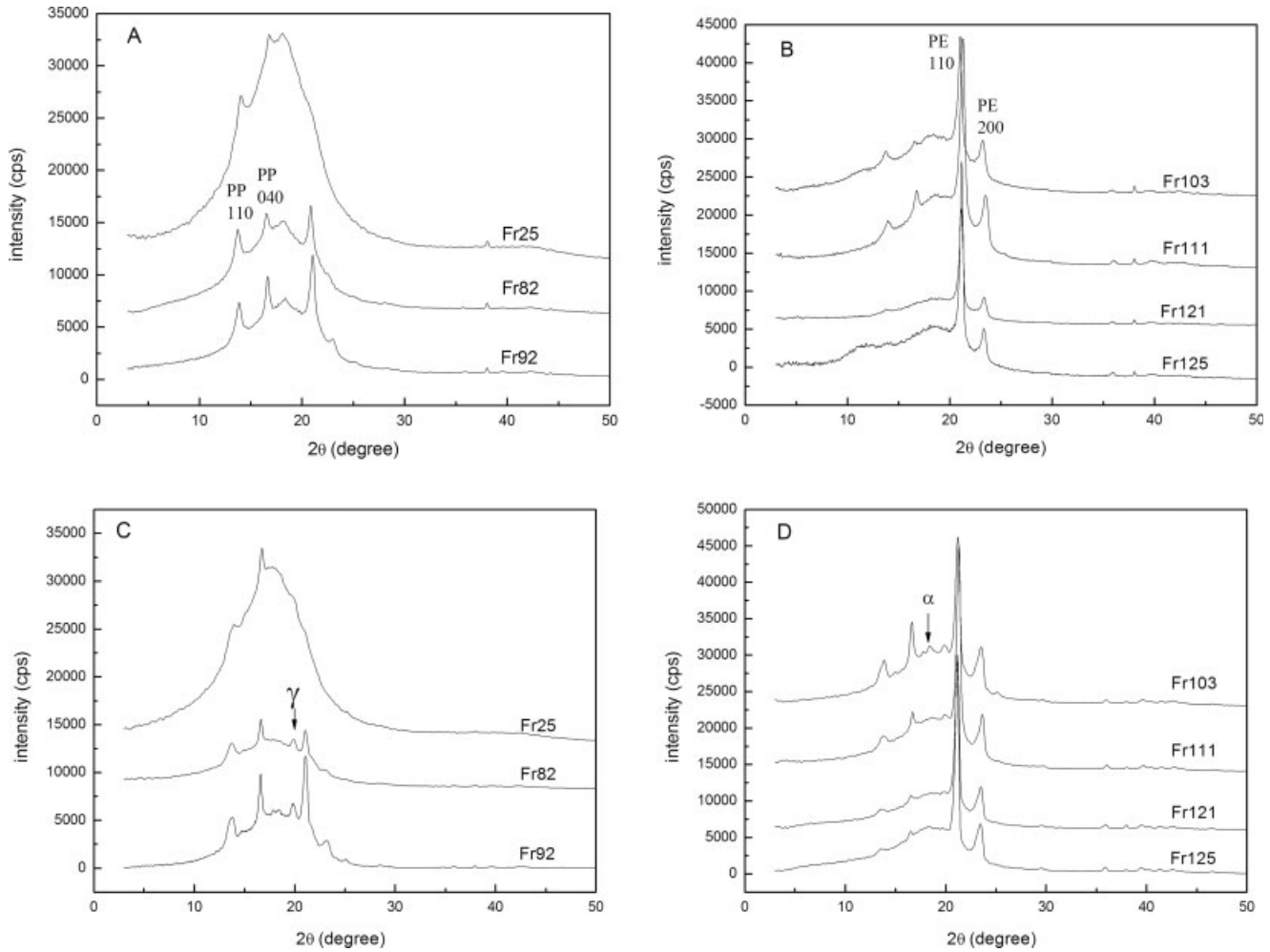

Figure 5 WAXD patterns of various fractions with two different thermal histories: (A,B) long-term storage at room temperature and (C,D) multistep crystallization.

Crystalline structures of the fractions

A WAXD analysis of the fractions was performed to evaluate the crystallization behavior of ethylene and propylene sequences and the effect of propylene sequences on the crystalline structure of the PE crystals. Two sets of samples with different thermal treatments (stepwise crystallization and room-temperature annealing) were used for WAXD experiments. Figure 5(A,B) shows WAXD patterns of the room-temperature-annealed fractions. Some relatively sharp peaks are superimposed on a broad, amorphous halo centered at $2\theta \approx 18.2^\circ$. This broad, amorphous halo is characteristic of EP random copolymers. As expected, for the high ethylene content fractions, an intensive peak at about 21° and a peak of moderate intensity at about 23° can be observed. These two peaks correspond to the (110) and (200) reflections of the orthorhombic PE crystal. For the low-ethylene-content fractions, the intensities of these two reflections decrease: the (200) reflection of Fr82 just appears as a shoulder, and for Fr25, even the (100) reflection almost disappears. On the other hand, for all the fractions measured, two peaks at about 13.8 and 16.6° can be observed as well, and they are assigned to the (110) and (040) reflections of the PP crystal, respectively. This shows that both ethylene and propylene sequences can crystallize and that PP crystals may also contribute to melting endotherms in the DSC curves. Now we can discuss the contents of PP crystals in different fractions. In the random EP component Fr25, the reflections of the PP crystal are also visible but very weak. Fr 82 and Fr92 exhibit the strongest PP reflections among these fractions, in accordance with their high [PPP] contents. Despite having the blockiest structure, fraction Fr111 contains less PP crystal because of its lower propylene content. With a further decrease in the propylene content, the length and number of successive propylene sequences decrease, and the reflections of PP crystals become even weaker.

The WAXD patterns of the fractions after stepwise crystallization are illustrated in Figure 5(C,D).

Comparing them with the room-temperature-annealed fractions, one can observe some differences for the fractions treated by stepwise crystallization. First, the (117) reflection of the γ-form PP crystal can be observed at 19.7° in some fractions, such as Fr82, Fr92, and Fr103. Early studies have indicated that the γ form is generally formed from short propylene sequences.[26–29] In fact, such short propylene sequences are always present in the c-EP component. The γ-form PP crystals are not observed in the room-temperature-annealed fractions, probably because the very short ethylene sequences distributed between propylene sequences can also be included in the PP crystals at a fast cooling rate. As a result, the propylene sequences may not be interrupted by the very short ethylene sequences, and thus α-form PP crystals are still formed. During stepwise crystallization, these very short ethylene sequences can be repulsed from the PP crystals as defects; then, γ-form PP crystals are formed. Second, we notice a distinct difference in the intensities of the PP reflections between the room-temperature-annealed and stepwise crystallized Fr103, whereas there is only a small difference for the other fractions between these two thermal treatments. We know from the ^{13}C-NMR data that Fr111 has the blockiest structure, and starting from this fraction, the length and number of successive propylene sequences decrease gradually with an increase in the ethylene content. It is possible that Fr103 contains lots of propylene sequences with a critical length. These propylene sequences can either be included in the PE crystals at a fast cooling rate or crystallize themselves under stepwise crystallization conditions. From the WAXD results, one can see that short propylene sequences can be included in PE crystals, and short ethylene sequences can also be included in PP crystals, depending on the sequence length and crystallization conditions.

The effect of propylene sequences on the *d*-spacing of reflections of PE crystals was also investigated. Generally, the inclusion of propylene units in PE crystals can cause expansion of the lattice. It has been reported that the *d*-spacing increases linearly with the propylene content for EP copolymers with low propylene contents.[30] However, there has been no report on the expansion of the PE crystal lattice in a copolymer with a high propylene content. Figure 6 shows the *d*-spacing of (110) and (200) reflections of PE crystals for the room-temperature-annealed and stepwise crystallized fractions. Fr111 has the smallest *d*-spacing values for both (110) and (200) reflections. This indicates that fewer propylene units are included in the PE crystals in this fraction than in the other fractions. ^{13}C-NMR data show that fraction Fr111 has the blockiest structure among these fractions, and this means that this fraction contains the fewest short sequences. Therefore, we can

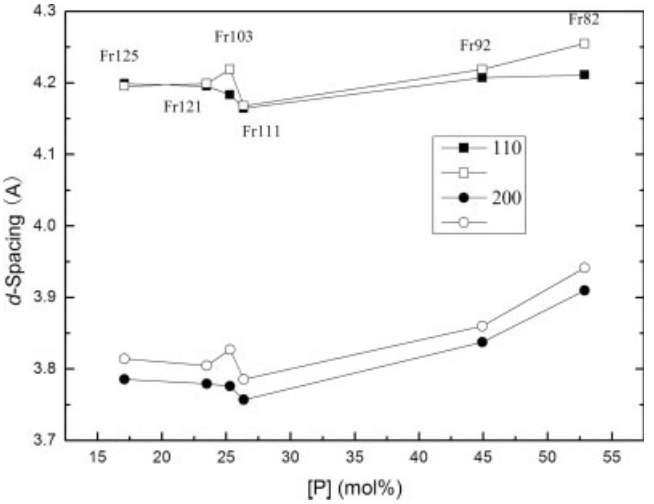

Figure 6 Dependence of the *d*-spacing values of the PE orthorhombic lattice on the composition of EP samples after step crystallization (filled symbols) and room-temperature annealing (open symbols) from the (110) and (200) reflections, respectively.

observe that the *d*-spacing of the (110) and (220) reflections decreases as the ethylene content increases at first and reaches a minimum at Fr111, and then it increases as the ethylene content further increases. Crystallization conditions also affect the expansion of the crystal lattice. The values of the *d*-spacing are usually smaller for the stepwise crystallized fraction because more propylene units are excluded from PE crystals under stepwise crystallization conditions. However, we have noticed abnormal values of the *d*-spacing for room-temperature-annealed Fr103: they are larger than those of both room-temperature-annealed Fr121 and room-temperature-annealed Fr111, although the ethylene content of F103 is between that of Fr121 and Fr111. In contrast, under stepwise crystallization conditions, the values of the *d*-spacing of Fr103 are between those of Fr121 and Fr111. As mentioned previously, Fr103 may contain many propylene sequences with a critical length that can either be included in PE crystals or crystallize themselves, depending on the crystallization conditions. In the room-temperature-annealed Fr103, these propylene sequences with a critical length tend to be included in PE crystals, thus leading to an abrupt increase in the *d*-spacing.

CONCLUSIONS

The experimental results show that an EP copolymer synthesized by a heterogeneous Ziegler–Natta catalyst system exhibits both intermolecular and intramolecular heterogeneity. The fraction of the largest quantity in EP sample Fr25 is basically a random copolymer, whereas the crystalline fractions tend to

become blocky as the ethylene content in the fractions increases. A further increase in the ethylene content leads to a decrease in the length and number of successive propylene sequences. The presence of multiple active centers in heterogeneous the Ziegler–Natta catalyst should account for the tremendous heterogeneity.

Thermal fractionation of the copolymer sample by stepwise crystallization has successfully resolved the DSC curves into multiple endotherms, and this indicates that even a single fraction comprises crystallizable sequences of different lengths. WAXD measurements reveal that there exist both crystallizable propylene and ethylene sequences in most of the fractions. Short propylene sequences can be included in PE crystals, and short ethylene sequences can also be incorporated into PP crystals. The incorporation of propylene sequences into PE crystals strongly depends on the sequence distribution and crystallization conditions. The number of propylene units incorporated into PE crystals is lowest in fractions with the blockiest structure.

References

1. Karian, H. G. Handbook of Polypropylene and Polypropylene Composites; Marcel Dekker: New York, 2003.
2. Strate, G. V. Encyclopedia of Polymer Science and Engineering; Wiley: New York, 1986; Vol. 6.
3. Fan, Z. Q.; Zhang, Y. Q.; Xu, J. T.; Wang, H. T.; Feng, L. X. Polymer 2001, 42, 5559.
4. Nomura, T.; Nishio, T.; Fujii, T.; Sakai, J.; Yamamoto, M.; Uemura, A.; Kakugo, M. Polym Eng Sci 1995, 35, 1261.
5. Doi, Y. Makromol Chem Rapid Commun 1982, 3, 635.
6. Cozewith, C. Macromolecules 1987, 20, 1237.
7. Fan, Z. Q.; Feng, L. X.; Yang, S. L. J Polym Sci Part A: Polym Chem 1996, 34, 3329.
8. Suhm, J.; Heinemann, J.; Worner, C.; Muller, P.; Stricker, F.; Kressler, J.; Okuda, J.; Mulhaupt, R. Macromol Symp 1998, 129, 1.
9. Wild, L.; Glöckner, G. Adv Polym Sci 1991, 98, 1.
10. Xu, J. T.; Feng, L. X. Eur Polym J 2000, 36, 867.
11. Pizzoli, M.; Righetti, M. C.; Vitali, M.; Ferrari, P. Polymer 1998, 39, 1445.
12. Shin, Y. W.; Uozumi, T.; Terano, M.; Nitta, K. H. Polymer 2001, 42, 9611.
13. Gan, S.; Burfield, D. R.; Soga, K. Macromolecules 1985, 18, 2684.
14. Greco, R.; Mancarella, C.; Martuscelli, E.; Ragosta, G.; Yin, J. Polymer 1987, 28, 1929.
15. Sworen, J. C.; Smith, J. A.; Wagener, K.; Baugh, L. S.; Rucker, S. P. J Am Chem Soc 2003, 125, 2228.
16. Guerra, G.; De Ballesteros, O. R.; Venditto, V.; Galimberti, M.; Sartori, F.; Pucciariello, R. J Polym Sci Part B: Polym Phys 1999, 37, 1095.
17. Alamo, R. G.; VanderHart, D. L.; Nyden, M. R.; Mandelkern, L. Macromolecules 2000, 33, 6094.
18. Hosier, I. L.; Alamo, R. G.; Esteso, P.; Isasi, J. R.; Mandelkern, L. Macromolecules 2003, 36, 5623.
19. Dong, Q.; Li, N.; Wang, X. F.; Fu, Z. S.; Xu, J. T.; Fan, Z. Q. Stud Surf Sci Catal 2006, 161, 25.
20. Jiang, T.; Chen, W.; Zhao, F.; Liu, Y.; Wang, R.; Du, H.; Zhang, T. J Appl Polym Sci 2005, 98, 1296.
21. Sacchi, M. C.; Fan, Z. Q.; Forlini, F.; Tritto, I.; Locatelli, P. Macromol Chem Phys 1994, 195, 2805.
22. Randall, J. C. J Polym Sci Part A: Polym Chem 1998, 36, 1527.
23. Carman, C. J.; Wilkes, C. E. Rubber Chem Technol 1971, 44, 781.
24. Wright, K. J.; Lesser, A. J. Macromolecules 2001, 34, 3626.
25. Alamo, R. G.; Chan, E. K. M.; Mandelkern, L.; Voigt-Martin, I. G. Macromolecules 1992, 25, 6381.
26. Turner-Jones, A. Polymer 1971, 12, 487.
27. Thomann, R.; Semke, H.; Maier, R. D.; Thomann, Y.; Scherble, J.; Mulhaupt, R.; Kressler, J. Polymer 2001, 42, 4597.
28. Alamo, R. G.; Kim, M. H.; Galante, M. J.; Isasi, J. R.; Mandelkern, L. Macromolecules 1999, 32, 4050.
29. Thomann, R.; Wang, C.; Kressler, J.; Mulhaupt, R. Macromolecules 1996, 29, 8425.
30. Rabiej, S. Eur Polym J 2005, 41, 393.